Steam Gasification of Lignite in a Bench-Scale Fluidized-Bed Gasifier Using Olivine as Bed Material

Elisa Savuto [1,*], **Jan May** [2], **Andrea Di Carlo** [3], **Katia Gallucci** [3], **Andrea Di Giuliano** [3] **and Sergio Rapagnà** [1]

1 Faculty of Bioscience and Agro-food and environmental technology, University of Teramo, Via R. Balzarini 1, 64100 Teramo, Italy; srapagna@unite.it

2 Institute for Energy Systems and Technology, Technische Universität Darmstadt, Otto-Berndt-Straße 2, 64287 Darmstadt, Germany; jan.may@est.tu-darmstadt.de

3 Industrial Engineering Department, University of L'Aquila, Piazzale E. Pontieri 1, Monteluco di Roio, 67100 L'Aquila, Italy; andrea.dicarlo1@univaq.it (A.D.C.); katia.gallucci@univaq.it (K.G.); andrea.digiuliano@univaq.it (A.D.G.)

* Correspondence: esavuto@unite.it

Abstract: The gasification of lignite could be a promising sustainable alternative to combustion, because it causes reduced emissions and allows the production of syngas, which is a versatile gaseous fuel that can be used for cogeneration, Fischer-Tropsch synthesis, or the synthesis of other bio-fuels, such as methanol. For the safe and smooth exploitation of syngas, it is fundamental to have a high quality gas, with a high content of H_2 and CO and minimum content of pollutants, such as particulate and tars. In this work, experimental tests on lignite gasification are carried out in a bench-scale fluidized-bed reactor with olivine as bed material, chosen for its catalytic properties that can enhance tar reduction. Some operating parameters were changed throughout the tests, in order to study their influence on the quality of the syngas produced, and pressure fluctuation signals were acquired to evaluate the fluidization quality and diagnose correlated sintering or the agglomeration of bed particles. The effect of temperature and small air injections in the freeboard were investigated and evaluated in terms of the conversion efficiencies, gas composition, and tar produced.

Keywords: lignite; lignite gasification; fluidized-bed gasifier; olivine

1. Introduction

The environmental issues associated with global warming have resulted in a strong tendency towards the reduction of greenhouse gas emissions in the field of energy production. This trend has thus drawn attention to clean-coal technologies, such as gasification, which, compared to conventional combustion, can reduce CO_2 emissions by up to 90% [1,2]. The gasification process consists of partial oxidation of an organic feedstock that takes place at high temperatures (around 700–1200 °C) in the presence of a gasification agent (air, steam, oxygen, or a combination of these). Gasification consists of a combination of chemical processes, such as drying, pyrolysis, combustion, and partial oxidation. The main product is syngas, which is a mixture of gases with a high calorific value, typically composed of H_2, CO, CO_2, and CH_4. Some undesired products are also generated during the process, such as particulate, acid gases, and tars (condensable heavy hydrocarbons) [3], which have to be removed in order to make the gas usable for energy purposes or the production of base chemicals.

Gasification can be a promising option for exploiting abundant carbonaceous solid resources, such as lignite [4], for the production of a versatile fuel gas with a wide range of possible final uses. The product gas can in fact be used for the production of electricity in integrated gasification combined

cycle systems (IGCC) or fuel cells [5], or it can be exploited for the synthesis of liquid fuels [6] and Fischer-Tropsch synthesis [7,8], thus reducing imports of oil and natural gas from outside Europe and reducing emissions from the transport sector. Lignite, with its high heating value and low volatile content compared to biomass, could be a very suitable feedstock for the gasification process [9,10].

Olivine, a mineral mainly composed of magnesium, iron oxide, and silica, is used as an inventory of the fluidized-bed reactor, because of its advantageous qualities. As stated in the literature, olivine is recommended as bed material because of its reported activity in tar reduction, which is comparable to that of calcined dolomite. Furthermore, olivine has a stronger attrition resistance, compared to dolomite, which makes it more suitable as bed material [11,12].

Previous works have already reported lignite gasification in fluidized-bed reactors. Bayarsaikhan et al. studied lignite steam gasification (particles of 500–1000 μm) in a fluidized-bed reactor with a bed of silica and alumina in the range of temperatures of 850–950 °C [13]. Additionally, Kern et al. investigated lignite gasification (particles of 2–6 mm) in the dual fluidized-bed gasifier developed by Vienna University with olivine as bed material, at an operating temperature of 850 °C, with steam/fuel ranging from 0.9 to 1.4 [14]. Furthermore, Karimipour et al. performed a statistical analysis based on the experimental results of lignite gasification (particles of 70–500 μm) in a fluidized-bed reactor of silica sand particles with steam and oxygen as oxidizing agents [15].

The novelty of the present work is the assessment of the fluidized-bed technology for the steam gasification of small particle size lignite (around 50 μm) pre-treated by the WTA process (fluidized-bed drying process with internal waste heat utilization, in german: Wirbelschichttrocknung mit interner Abwärmenutzung), with a bed of olivine particles in a temperature range of 750–850 °C and a steam/fuel ratio equal to 0.65. Furthermore, in this work, the operating temperature was changed in order to study its effect on the gas quality, and in some of the experimental tests, air injections were added in the freeboard, in order to reproduce, on a smaller scale, the oxygen added in the post gasification zone of the High Temperature Winkler (HTW) gasifier [2,16], and thus to assess its effectiveness in tar reduction.

This work was carried out within the European project LIG2LIQ [17], whose aim is to develop an economically efficient concept for the production of liquid fuels, such as Fischer-Tropsch fuels or methanol, from lignite and solid recovered fuel from municipal waste by means of HTW gasification technology. Therefore, in the first step, the concept of HTW gasification, which was optimized with respect to the cold gas efficiency and carbon conversion efficiency, using lignite/waste mixtures as feedstocks for the production of syngas, was studied on a small scale. This paper describes the results of gasification experiments using only lignite as fuel in a laboratory fluidized bed. In the second step, experiments with a mixture of municipal waste and lignite were carried out.

Lignite gasification tests were carried out in a bench-scale fluidized-bed reactor, with the aim of investigating the best conditions to produce a high-quality syngas, with a low tar content and high H_2 and CO fraction, foreseeing downstream processes for Fischer-Tropsch or methanol synthesis. Tests were carried out, as mentioned above, changing the operating temperature and carrying out small air injections in the freeboard of the gasifier, in order to study the effect of a temperature increase in the upper part of the reactor aimed at enhancing tar conversion. The results were evaluated in terms of the syngas composition, tar content, gas yield, and conversion rates. Additionally, pressure fluctuation signals were acquired in the reactor freeboard during experimental tests, in order to evaluate the fluidization quality at the explored process conditions and to detect possible sintering or particle agglomeration within the bed inventory; in fact, these phenomena can increase the particles' average diameter, and then negatively affect the fluidization properties [18].

Therefore, the aim of the work was to evaluate the quality of the product gas obtained from the gasification of fine lignite in a fluidized bed of olivine particles at different temperatures, and to study the effect of air injections in the enhancement of tar reduction. In addition, the analysis of the materials before and after tests and the pressure fluctuation analysis helped to assess the eventuality of

undesired phenomena, such as ash melting and the aggregation of bed particles, which could lead to defluidization of the bed.

2. Materials and Methods

2.1. Experimental Test Rig

The bench-scale gasification reactor represented in Figure 1 was used to carry out the experimental tests. The gasifier consisted of a cylindrical stainless steel reactor (internal diameter of 100 mm and height of 850 mm) externally heated with a 6 kW electric furnace. Steam was used as a gasification agent and a flow of nitrogen was added in order to fluidize the bed; they were sent to a wind-box to be mixed and pre-heated, and then fed from the bottom of the gasifier through a porous ceramic distribution plate. In order to investigate the effect of an increase of temperature in the freeboard, in some tests, a small stream of air was injected in the freeboard through a steel tube of a 6 mm diameter. The bed material used was sintered, calcined olivine particles provided by Magnolithe GmbH [19] with a $d_{3,2}$ diameter of 317 μm and density of 3000 kg/m^3, with the following composition by weight: MgO, 48%–50%; SiO_2, 39%–42%; and Fe_2O_3, 8%–10%. As reported in the literature, calcination at high temperatures (around 1100 °C or higher) allows the iron oxides contained in the olivine particles to emerge at the surface, and thus to be available for catalytic reactions [20–22]. The height of the bed in the reactor was approximately 200 mm. The feedstock consisted of WTA lignite, and Rhenish lignite from a process of fluidized-bed drying with internal waste heat utilization [23], supplied by RWE Power AG. Lignite was continuously fed to the bed of the reactor by means of a screw feeder and a feeding probe that delivered the material directly to the fluidized bed. The feeding probe was purged with a small N_2 flow, in order to help the fall of the feedstock and to avoid the material from clogging the tube. The reactor was designed to host a ceramic filter candle in the freeboard above the bed, through which the product gas was forced to pass to exit the gasifier; in this way, the solid particulate remained on the external surface of the candle and the dust-free gas could exit the reactor.

The product gas downstream of the gasifier was sent to heat exchangers for gas cooling and condensation of the residual steam. Circulation of the gas was granted by a vacuum pump. The flow of the dry product gas was measured with a mass flow controller, and its composition was analysed by online gas analyzers; a slipstream of the gas produced, about 1 Nl/min, was sent to the tar sampling unit, carried out following the specification of the standard CEN/TS 15439. The gas passed through five impinger bottles containing 2-propanol and kept in a cold bath at −20°C, to help the condensation of tars. The gas stream was moved by a vacuum pump and its flow rate was controlled by a mass flow controller. Finally, the main gas stream and the slipstream used for tar sampling were both sent to the vent.

Temperatures were measured by means of three K-type thermocouples: one was positioned in the reactor bed (T1); one was located in the freeboard (T2); and the other was situated at the exit of the candle, just at the outlet of the filter (T3). The operating temperature was considered the average of the values measured from T1, T2, and T3. Differential pressures were measured by means of pressure probes through the candle (ΔP1) and through the reactor (ΔP2). The pressure probes were connected to U-tube manometers, and were able to measure in the range of 0.5–90 mbar.

The fluidized-bed bench-scale reactor was equipped with a vertical probe in its freeboard, for acquisitions of pressure fluctuation signals. The probe was connected to a piezoelectric pressure transducer, in turn transmitting its signal to a charge amplifier KISTLER 5019A, and the operation parameters were tuned so as to obtain the highest amplification, without overloading. The resulting amplified voltage signal was then digitally converted and stored on a PC, provided with a tailored LABVIEW® routine. The data acquisition frequency was 100 Hz, which is much higher than the values typically observed in gas-fluidized beds under study (less than 10 Hz). The duration of each acquisition was 2–3 min, to ensure their repeatability and significance [24]. Stored signals were processed by means of a MATLAB® script, which calculated their standard deviations, as well as the power spectral

density function (PSDF), by fast Fourier transform [25]. Standard deviations are directly related to the size of bubbles erupting at the upper bed surface (the higher the standard deviation, the bigger the bubbles), while PSDF allows dominant frequencies of pressure fluctuations to be identified, related to the number of erupting bubbles [18].
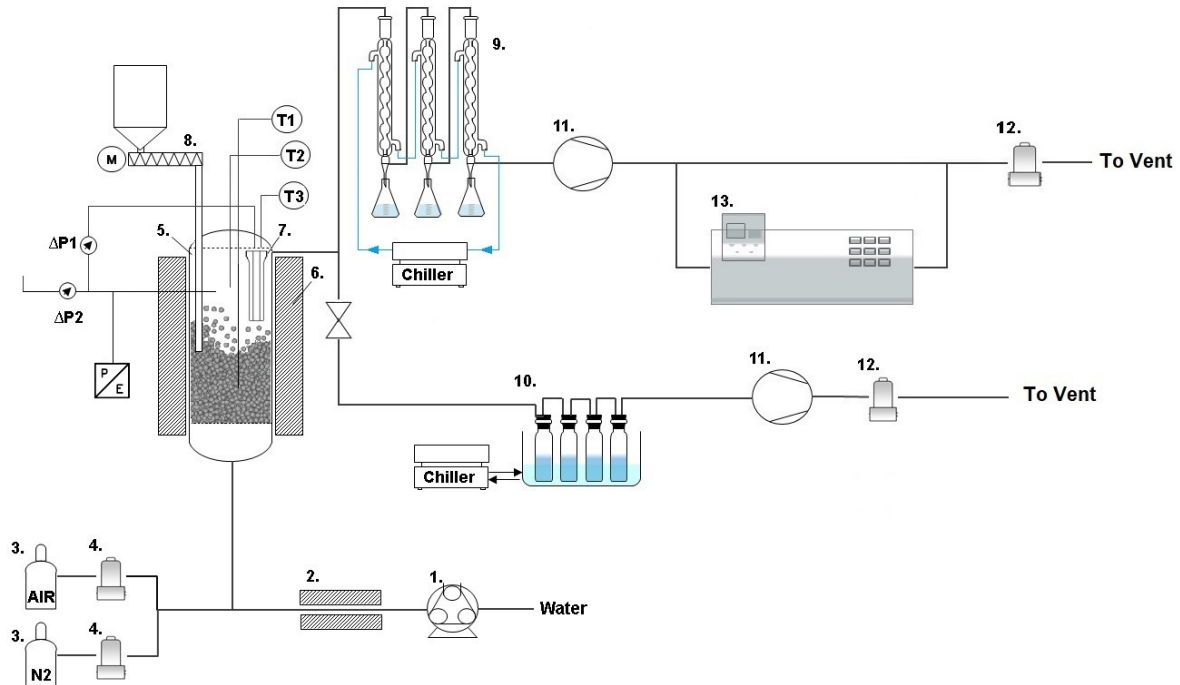
Figure 1. Scheme of the bench-scale gasification test rig. 1—water pump; 2—steam generator; 3—air and N_2 gas tanks; 4—air and N_2 mass flow controllers; 5—bubbling fluidized-bed gasifier; 6—electric furnace; 7—ceramic filter candle (OD of 60 mm, length of 440 mm); 8—screw conveyor for feeding fuel; 9—heat exchangers for steam condensation; 10—tar sampling unit; 11—vacuum pumps; 12—syngas mass flow controllers; 13—gas analyzers.

The lignite gasification tests were carried out using olivine as bed material, with a constant feeding rate of lignite and steam. For each test, a new batch of calcined olivine was inserted as bed material in the reactor, in order to compare tests with equivalent initial conditions avoiding the accumulation of ash in the bed material, which could have beneficial effects, such as the enhancement of tar conversion [26,27]. The operating temperature was changed in the tests between 750 and 850 °C and air injections were added in three of the six tests. Tests #1, #2, and #3 were carried out at operating temperatures of approximately 750, 800, and 850 °C, respectively. Tests #4, #5, and #6 had the same input conditions adopted in the first three tests, but with an additional air stream of 8 Nl/min injected in the freeboard of the reactor.

The operating conditions used are summarized in Table 1.

Table 1. Operating conditions of the test campaign.

Test	#1	#2	#3	#4	#5	#6
Feedstock (g/min)				12.75		
Operating Temperature (°C)	750	800	850	750	800	850
Air Injections (Nl/min)	-	-	-	8	8	8
Steam flow (g/min)				8.25		
N_2 flow (Nl/min)	8.83	17.20	7.39	7.32	7.44	7.44
Steam/Fuel (g/g)				0.65		

2.2. Analysis of Products

Downstream of the steam condensers and the vacuum pump, a slipstream of the product gas was sent to online gas analyzers for an evaluation of the composition. Online analyzers allowed H_2, CO, CO_2, CH_4, H_2S, and NH_3 to be detected (ABB URAS, LIMAS, CALDOS, and ULTRAMAT 6 Siemens).

The water content in the product gas was calculated from the quantity of water collected in the flasks connected to the steam condensers. The water conversion η_{wc} (%) was thus calculated as

$$\eta_{wc} = \frac{\dot{m}_{water,\,in} - \dot{m}_{water,\,out}}{\dot{m}_{water,\,in}} \times 100, \tag{1}$$

where $\dot{m}_{water,\,in}$ and $\dot{m}_{water,\,out}$ are the mass flows of the water input and output, respectively.

The quantity of dry product gas, measured by means of a mass flow controller, allowed the gas yield Y_{gas} $\left(Nm^3/kg_{feedstock}\right)$ to be calculated:

$$Y_{gas} = \frac{F_{gas,\,out}}{F_{feedstock,\,in}}, \tag{2}$$

where $F_{gas,\,out}$ is the total dry N_2-free volume of gas flow produced, and $F_{feedstock,\,in}$ is the mass flow of the input feedstock.

From the analysis of the gas composition and the carbon content in the feedstock, it was possible to calculate the carbon conversion X_C (%):

$$X_C = \frac{n_{CO} + n_{CO_2} + n_{CH_4}}{n_{C_{in}}} \times 100, \tag{3}$$

where n_i represents the moles of the i carbonaceous species in the product gas (CO, CO_2, and CH_4), and $n_{C_{in}}$ represents the total moles of C in the feedstock input.

Post-combustion was carried out after gasification: an air stream was fed to the reactor and the gaseous products (CO and CO_2) were analysed and quantified, in order to evaluate the amount of the residual un-reacted char in the reactor. From this result, it was possible to calculate the char yield Y_{char} (%):

$$Y_{char} = \frac{m_{char}}{m_{feedstock}} \times 100, \tag{4}$$

where m_{char} is the mass of the residual char estimated by the post-combustion in the gasifier, and $m_{feedstock}$ is the mass of the total feedstock fed.

The cold gas efficiency η_{CG} (%) was calculated as

$$\eta_{CG} = \frac{LHV_{gas} F_{gas,\,out}}{LHV_{lignite} F_{feedstock,\,in}}, \tag{5}$$

where LHV_{gas} and $LHV_{lignite}$ are the lower heating values of the gas produced and lignite, expressed in MJ/Nm^3 and MJ/kg, respectively.

The liquid tar samples collected in the impinger bottles were analysed offline by means of HPLC (Hitachi "Elite LaChrom" L-2130) for the detection and quantification of heavy hydrocarbons in the product gas. The tar compounds chosen as representative of a typical tar composition [28] were as follows: phenol, toluene, styrene, indene, naphthalene, acenaphthylene, fluorene, phenanthrene, anthracene, fluoranthene, and pyrene.

After each test, the bed material was extracted from the reactor and sieved, in order to separate the fly-ashes accumulated in the bed during the experimental run from the olivine particles; samples of ashes were thus collected for analysis after tests. Afterwards, the ashes were analysed by means of SEM/EDS and XRD analyses, in order to study their morphology and the present elements and compounds.

3. Results and Discussion

3.1. Analysis of Materials Pre-Test

3.1.1. Lignite

The characterization of lignite, supplied by Technische Universität Darmstadt (TUDA), and its particle size distribution, are reported in Table 2 and Figure 2, respectively. The particle size analysis was performed with a Malvern Mastersizer 2000.

Table 2. Proximate and ultimate analysis of lignite.

	Weight %
Total Moisture content (%)	16.09
Ash content (dry basis) (%)	13.86
Volatile matter (dry basis) (%)	38.57
C (dry basis) (%)	67.51
H (dry basis) (%)	4.88
N (dry basis) (%)	0.76
S (dry basis) (%)	1.11
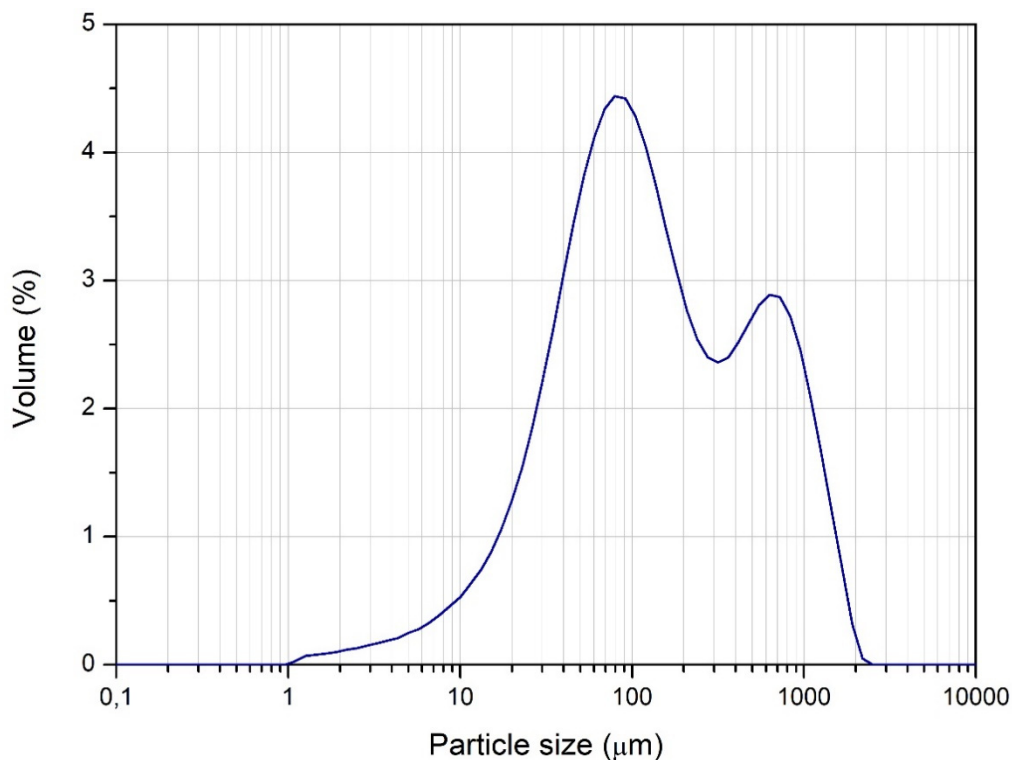
Figure 2. Particle size distribution of lignite.

Figure 2 shows that lignite has a bimodal particle size distribution, meaning that there are two main particle diameters: a high content of particles with a smaller diameter (around 70 μm) and another relevant fraction of particles with a larger diameter (around 600 μm). The $d_{3,2}$ diameter of lignite given by the particle size analysis is 44.08 μm.

As the average diameter of the feedstock particles is very small, working with the filter candle in the freeboard of the gasifier is recommended, in order to avoid the entrainment of lignite particles outside of the reactor with the gas flow.

3.1.2. Olivine before Tests

The particle size analysis of olivine before the gasification tests is reported in Figure 3.
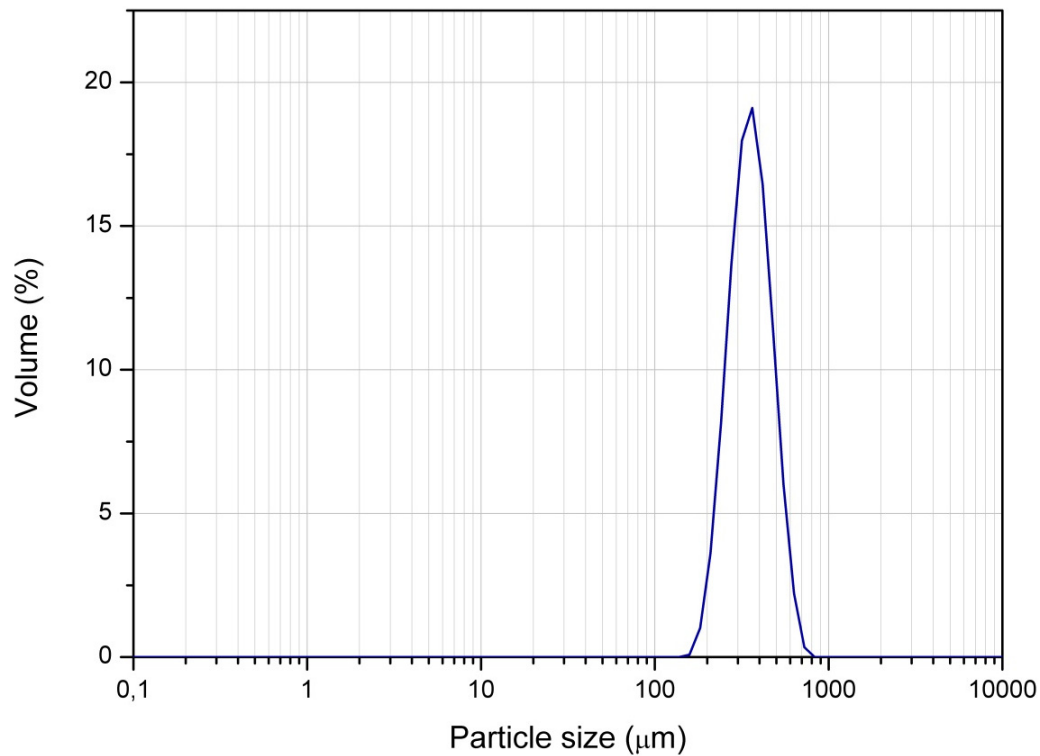

Figure 3. Particle size distribution of olivine.

The $d_{3,2}$ diameter of olivine given by the particle size analysis is 316.75 µm.

3.2. Gasification Results

The results obtained are summarized in Table 3.

Table 3. Results of lignite gasification tests.

Test	#1	#2	#3	#4	#5	#6
Bed Temperature (°C)	752	813	841	757	800	850
Avg Temperature (°C)	757	825	842	741	786	818
Air Injections (Nl/min)	-	-	-	8	8	8
Steam/Fuel	0.61	0.64	0.65	0.65	0.65	0.66
Length test (min)	120	120	120	121	66	50
H_2O conversion (%)	38.91	57.86	56.07	28.14	32.92	35.04
C conversion (%)	66.12	68.52	75.41	62.50	67.51	90.17
Gas yield (Nm^3/kg)	1.35	1.41	1.37	1.03	1.15	1.46
H_2 (%) dry N_2-free	55.11	54.28	53.16	49.78	49.38	48.48
CO (%)dry N_2-free	22.75	27.91	31.03	19.93	23.01	30.69
CO_2 (%) dry N_2-free	18.56	13.53	12.87	26.92	24.73	17.76
CH_4 (%) dry N_2-free	3.58	4.28	2.95	3.37	2.89	3.08
NH_3 (ppm) dry N_2-free	1094	1355	761	902	957	886
H_2 (Nl/min)	10.12	9.65	10.07	7.63	7.80	10.06
Char yield (%)	17.06	8.93	8.00	14.91	7.86	
η_{CG} (%)	57.11	61.27	58.21	44.58	42.17	58.94
Tar content (mg/Nm^3)	2461	938	481	2259	N.A.	305
Mass balance (err %)	1.25	6.11	4.95	3.25	5.62	

The length of tests #5 and #6 was shorter compared to the previous tests; however, the gas composition analysed online during the tests reached a steady state after around 10 min, giving stable values for the entire length of the test; a 60 min period was therefore considered sufficient for an evaluation of the results. The amounts of char and ash produced during gasification were evaluated in relation to the total amount of lignite fed during the experimental run. Consequently, the evaluation of their content was not affected by the length of the test.

From the comparison of the results obtained in the first three tests, it is possible to observe that, in general, at higher temperatures, the product gas has a higher quality in terms of the H_2O and C conversions and gas yield. Moreover, the gas composition in the tests carried out at 850 °C displays an increase in CO and decrease in CO_2, probably caused by the higher extent of steam gasification reactions that takes place for higher temperatures, and the lower extent of the WGS reaction, enhanced at lower temperatures (~600 °C). Starting from the syngas compositions obtained in the six experimental runs, the equilibrium contents of CO and CO_2 were calculated with the software Aspen Plus, in order to compare the experimental and equilibrium compositions. The equilibrium compositions calculated were approximately equal to the gas compositions obtained in the experimental tests, meaning that the WGS reaction had reached equilibrium. For higher temperatures, the char yield is also lower, which is proof of the higher conversion of carbon and thus lower amount of solid un-reacted residual char. Furthermore, the amount of tar produced at higher temperatures is lower compared to the cases with lower temperatures. In the tests conducted at 750 °C, the tar content is around 2.5 g/Nm^3, while at 850 °C, it reduces to 0.5 g/Nm^3. Regarding the tar content in general, it was observed that in tests with lignite, the amount of tar produced is lower compared to in similar tests carried out with biomass in the same experimental reactor with olivine as bed material [27,29,30]. Biomass gasification tests in similar conditions carried out at 800 °C produced tar contents ≥3300 mg/Nm^3, while lignite gasification at the same temperature (test #2) produced a tar content <950 mg/Nm^3. This phenomenon could be related to the lower volatile content of lignite compared to biomass (~50% versus ~70%, respectively [27]). In fact, volatile matter has been reported to make organic feedstocks more susceptible to tar formation [31].

The tests with and without air injections in the freeboard were evaluated in a comparison. As expected, in the tests with air injections, there is a higher content of CO_2 in the product gas. Furthermore, in the tests with air injections, the H_2O conversion was lower, probably because, being a product of combustion, it increases during the reaction. The H_2 content and its production in terms of Nl/min are lower compared to the case without air injection. It is possible that some of the produced H_2 was consumed in the combustion reactions with the injected O_2. The difference between the H_2 produced in test #2 (without air injections) and test #5 (with air injections), and their corresponding difference in H_2O content in the syngas are both in the order of 0.1 mol/min. This supports the hypothesis that the missing H_2 in the tests with air injections has been combusted and converted into additional H_2O, as confirmed by the consistency of the reported values of molar flows. In all of the tests, the H_2S content was approximately 400 ppm on a dry N_2-free basis. The NH_3 content, favored by the presence of steam as a gasification agent [32], was around 1000 ppm, with lower values at 850 °C. The higher NH_3 content at 800 °C, noticed both in the tests with and without air injections, was also observed by Xie at al. in gasification experiments on coal macerals [33], and could be related to the combination of two effects: the increase of NH_3 production from the N-containing structures in coal enhanced in steam gasification with a higher temperature [32,34,35], and the thermal decomposition of NH_3 occurring for increasing temperatures, as found in the literature [36]. For tests #4, #5, and #6, in which air was injected in the freeboard, the presence of O_2 increases the possibility of NH_3 combustion and consequently decreases its content in the product gas, showing the same trend as a function of temperature.

As mentioned above, in tests #4, #5, and #6, combustion of part of the gas took place, as expected, as a consequence of the air injections, especially those performed in order to increase the temperature in the freeboard and enhance the reactions of tar decomposition. In spite of the combustion reactions, it was observed that the tar content was not really affected by the air injections. The explanation for

this could be that in the bench-scale gasifier, the temperature of the reactor is controlled by the electric furnace, so the temperature increase caused by the combustion did not have a relevant effect for the promotion of the tar conversion reactions. In addition, due to the reduced dimensions of the bench-scale reactor, the air injections in the freeboard are close to the exit of the gasifier, and consequently, tars could have had too little residence time to decompose. Moreover, the high content of inert N_2 in the air injected, which dilutes the O_2, could be the cause of the attenuation of the temperature increase due to the combustion, thus reducing the beneficial effect of the air injections.

A global mass balance was carried out, taking into account the mass flows of lignite and steam as inputs for the duration of the test. The outputs were calculated as the sum of the masses of the gases produced, the liquid water condensed downstream of the reactor, the tar contents in the samples (reported as the total gas flow), the ash content separated and collected from the bed material after the tests, and the char and residual carbon in the reactor (including the carbon particles deposited on the surface of the filter candle), which were evaluated from the post-combustion carried out after each test.

3.3. Analysis of Materials after the Test

Lignite Ash

The ashes produced during the tests were collected and analysed with SEM/EDS. Figures 4 and 5 show that in some spots of the analysed areas, Si and Mg are found together, probably corresponding to olivine particles still present in the ashes after their separation from the bed material. Furthermore, it was noticed that Ca, which is largely present in lignite ashes [37,38], was often found together with S in some spots analysed, as highlighted by the colored maps showing the presence of single elements in the particles.

The ashes generated during the tests were also analysed with XRF and XRD. The elements detected and quantified with the XRF analysis are reported in Table 4. The value of loss of ignition was 43.28%. The result of the XRD analysis is reported in Figure 6.

The results of the XRF analysis show that the elements present in major quantities are Ca, S, Fe, Si, Mg, and Na, as observed in the results obtained from the SEM/EDS analysis.

Figure 6 shows the diffraction spectrum of the ashes collected in the reactor after gasification and post-combustion. The broad halo visible at low Bragg angles indicates the presence of amorphous phases typical of ashes [39]. The peaks identified show the presence of K and Ca oxides present in the ashes, and of Si, Mg, and Fe compounds, present in both the ashes and the olivine particles [40]. Furthermore, the phase $CaSO_4$ was identified, as proof of the affinity between Ca and S already observed in the results of the SEM/EDS analysis. The observation of Ca and S together, in the characterization analysis of the ashes, could be proof of the capacity of Ca to react with S, as reported in the literature [41,42], and thus to retain the sulphur compounds in the ashes.
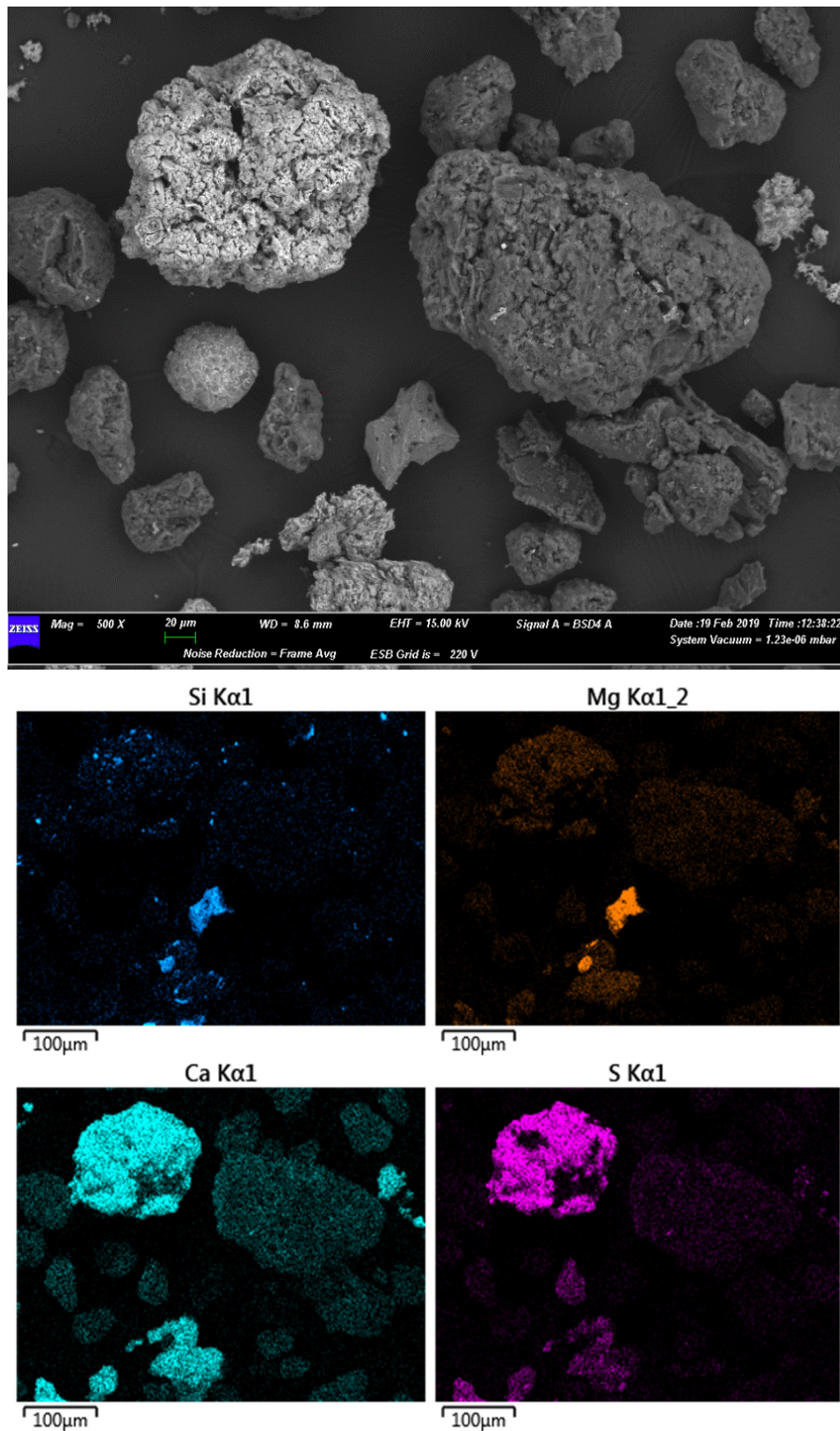
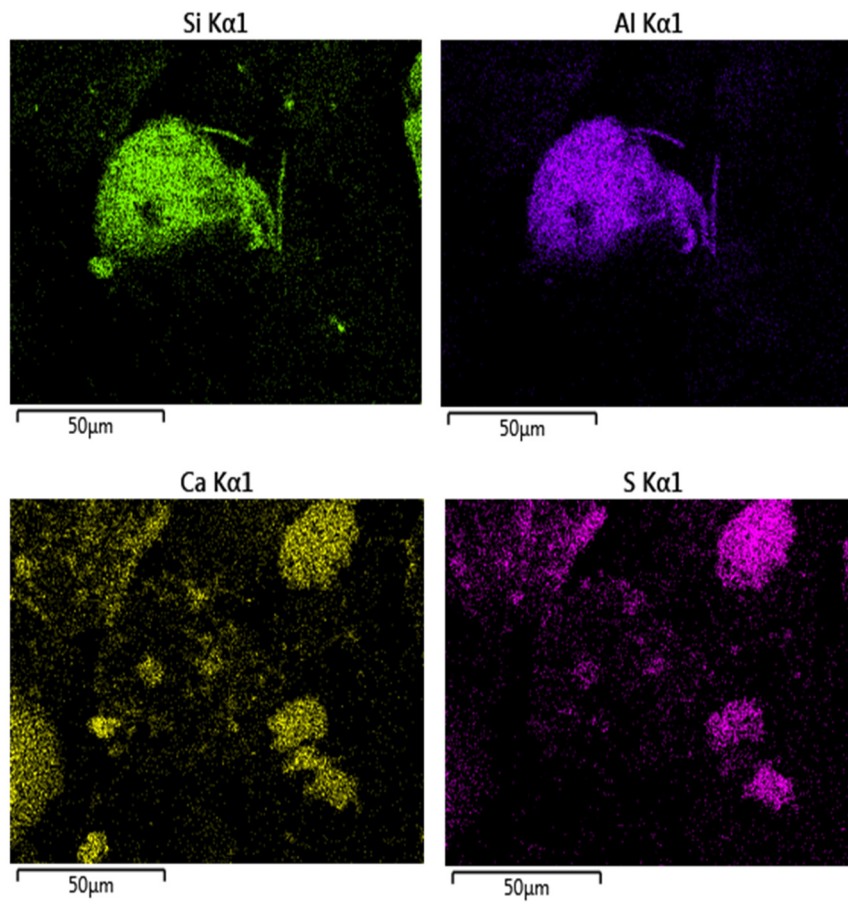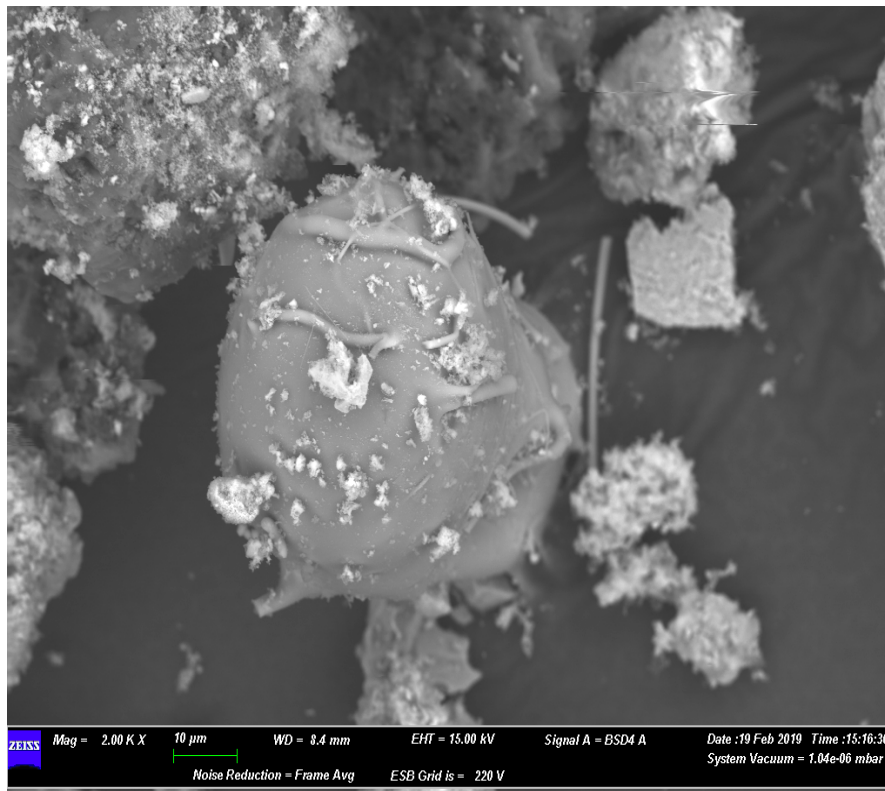**Figure 4.** SEM/EDS of ash from lignite (image 1).

Figure 5. SEM/EDS of ash from lignite (image 2).

Table 4. XRF analysis of lignite ash produced during the gasification test.

| Element	Concentration (%)	Absolute Error (%)
Na	0.705	0.037
Mg	2.399	0.016
Al	0.149	0.0046
Si	3.690	0.006
S	6.577	0.004
Cl	0.113	3×10^{-4}
K	0.094	0.0011
Ca	12.460	0.01
Ti	0.108	7×10^{-4}
Cr	0.072	2.5e-04
Mn	0.176	4×10^{-4}
Fe	5.964	0.005
Ni	0.067	3×10^{-4}
Cu	0.0143	1.4×10^{-4}
Sr	0.145	1×10^{-4}
Ba	0.169	0.0011
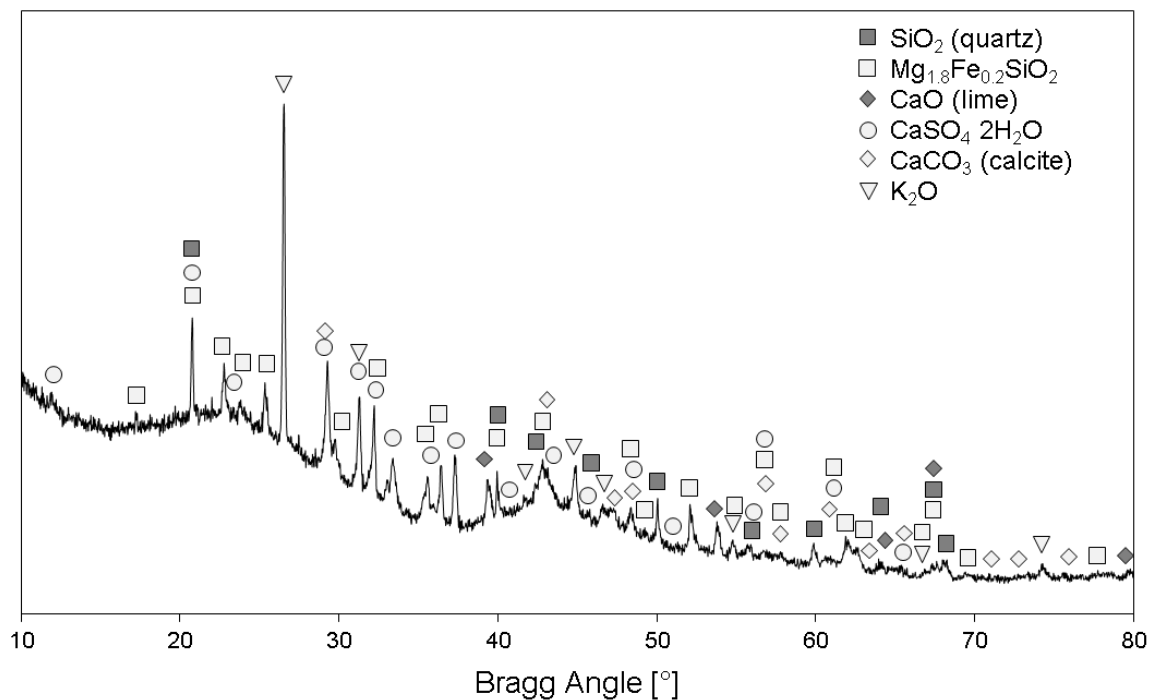
Figure 6. XRD analysis of lignite ash.

3.4. Pressure Fluctuation Analysis

More than 150 acquisitions of pressure fluctuation signals were performed during the six tests discussed above, always depicting the situation exemplified by Figure 7 for test #1. During the preliminary heating of the reactor, under an N_2 flowrate high enough to fluidize the bed, PSDF resulted in dominant frequencies of around 3–4 Hz (Figure 7a), which were compatible with the desired bubbling fluidization regime (usually less than 10 Hz) [24] and were assumed to be characteristic of the fresh olivine bed inventory. As soon as the gasification session started, a series of low-frequency phenomena (<1 Hz) took action with a high power spectral density, partially disguising those related to bed bubbles in the PSDF; the latter were still detectable, maintaining their dominant characteristic frequencies at 3–4 Hz (Figure 7b). The low-frequency phenomena were associated with the peristaltic pump feeding water and the instantaneous devolatilization of lignite particles. As further confirmation

of this last observation, pressure fluctuation signals were also acquired during post-combustion, when water and lignite were no longer fed. In related PSDF, dominant frequencies clearly reappeared within the range of 3–4 Hz, without any high power spectral density disturbance at less than 1 Hz (Figure 7c).
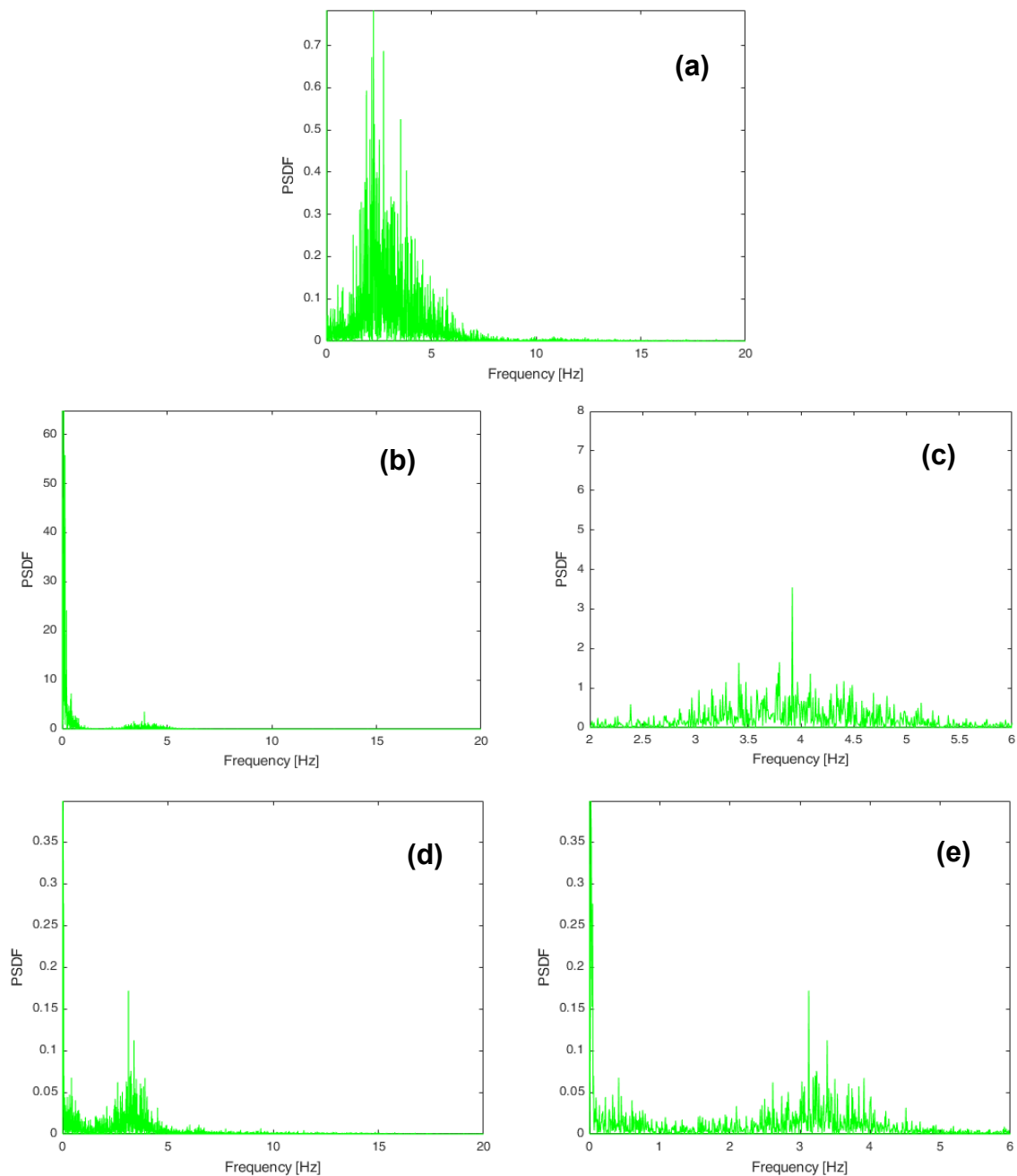
Figure 7. Power spectral density function (PSDF) of pressure fluctuations signals from test #1: pre-heating under N_2, T = 767 °C (**a**); gasification (**b**) with magnification of a 2–6 Hz range (**c**); and post-combustion (**d**) with magnification of a 0–6 Hz range (**e**).

For the case shown in Figure 7, standard deviations of pressure fluctuation signals were 0.98 mbar for preliminary heating (Figure 7a), 3.14 mbar during gasification (Figure 7b), and 0.39 mbar for post-combustion (Figure 7c), with trends and orders of magnitude representative of all tests. The fresh olivine beds during preliminary heating, approaching temperatures of the gasification, had pressure fluctuations with a standard deviation of around 1 mbar. It increased several times during gasification

(because of the powerful low-frequency phenomena mentioned above), and then returned to the order of 1 mbar in the post-combustion phase.

All these observations allowed us to conclude that, for the investigated process conditions, the olivine bed inventory did not undergo modifications able to modify its fluidization quality, as sintering between olivine particles or due to lignite and ashes. This would have caused an increase of the average particle diameter and then a drop in the fluidization quality, detectable by PSDF modifications. SEM analyses confirmed the absence of particle sintering or agglomeration. Figure 8 shows an SEM image of olivine after the test, in which it is possible to see that the dimensions of the particles are approximately between 200 and 400 μm, similar to the particle size of olivine before the test. No sign of agglomeration or particle sintering is observed from the SEM images. In the tests carried out in this work, the absence of agglomeration issues was probably proof of the suitability of the operating temperatures chosen, which were lower than the ash melting point. Furthermore, fluidized-bed technology has the well-known advantage of guaranteeing a good mixing of the materials and thus a uniform distribution of temperatures across the reactor volume, avoiding the presence of hot spots that could be responsible for ash melting.

The evaluation of the agglomerate formation for longer operational times, and therefore with an increased ash content due to accumulation, was not taken into account, because the tests carried out in this work aimed to reproduce the operation of the HTW gasifier, in which the ash produced during the process is discharged from the bottom of the reactor [43], and consequently, the accumulation of high contents of ash does not take place.
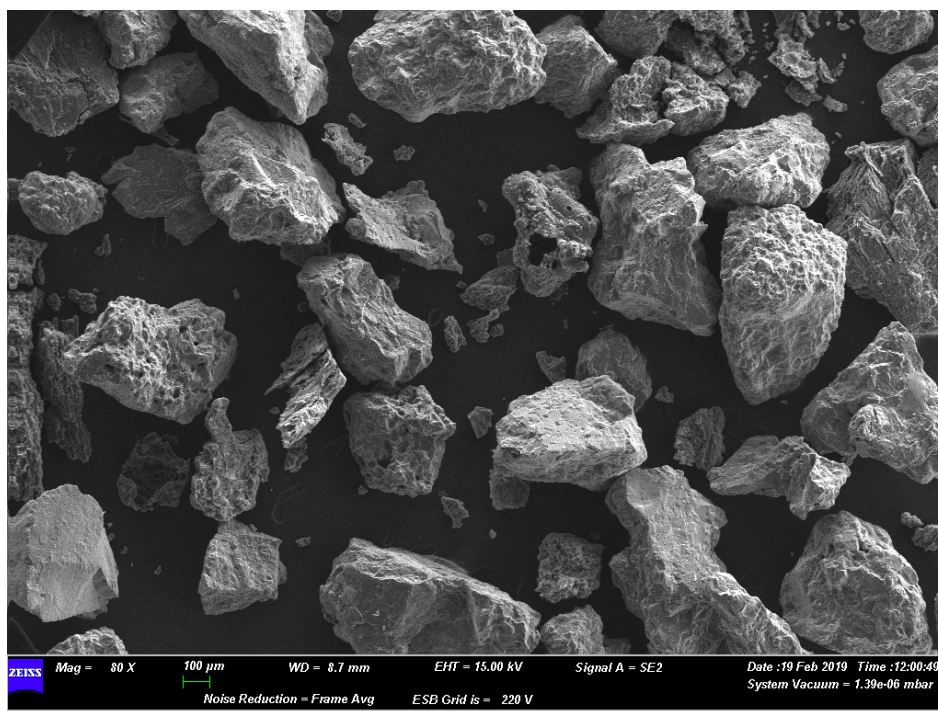

Figure 8. SEM analysis of olivine after the test.

4. Conclusions

Steam gasification tests with lignite were carried out in a bench-scale fluidized-bed gasifier, in order to study the quality of the gas produced at different operating conditions. The correct operation of the gasification process with small lignite particles as feedstock (~44 μm) was possible thanks to the ceramic filter candle integrated in the freeboard of the gasifier, which prevented the entrainment of particles outside the reactor. The bed material used was olivine, and the Steam/ Fuel ratio (S/F)

was kept at approximately 0.65. The effect of the temperature and air injections in the freeboard was investigated in terms of the gas composition and tar produced.

The results obtained showed that the increase of the operating temperature caused an improvement of the gas quality, in particular, higher conversion rates and gas yields, and a lower amount of tar produced. Tests carried out with air injections in the freeboard did not show the desired effect of tar reduction, probably because the combustion of part of the syngas did not cause the increase of temperature expected in the externally heated bench-scale gasifier used in this work. However, the amount of tar produced was smaller compared to other tests carried out with biomass at similar operating conditions in the same bench-scale gasifier. Lignite could be less prone to tar production because of its lower volatile content compared to lignocellulosic biomass.

The ashes produced during the gasification test were analysed with XRD and SEM/EDS analysis, and an affinity between Ca and S was noticed, probably indicating the capacity of Ca to retain S in the ashes.

Pressure fluctuations were acquired in the freeboard of the fluidized bed during each test, in order to diagnose possible alterations in the fluidization quality, related to sintering phenomena involving bed particles. The results from the signal analyses, in terms of dominant frequencies in the power spectral density functions and standard deviations, did not show any worsening of the fluidization quality for all investigated gasification conditions. This was confirmed by the SEM analysis, which did not exhibit clusters of particles.

Conflicts of Interest: The authors declare no conflicts of interest. The funders had no role in the design of the study; in the collection, analyses, or interpretation of data; in the writing of the manuscript, or in the decision to publish the results.

Abbreviations

IGCC	Integrated Gasification Combined Cycle
HTW	High Temperature Winkler
OD	Outer Diameter
WTA	Fluidized-bed drying process with internal waste heat utilization (German: Wirbelschichttrocknung mit interner Abwärmenutzung)
HPLC	High Performance Liquid Chromatography
Avg	Average
PSDF	Power Spectral Density Function
S/F	Steam to Fuel
N.A.	Not Available
XRD	X-ray Diffraction
XRF	X-ray fluorescence
SEM	Scanning Electron Microscope
EDS	Energy-dispersive X-ray Spectroscopy

Symbols

η_{wc}	Water conversion
$\dot{m}_{water,\,in}$	Mass flow of water input
$\dot{m}_{water,\,out}$	Mass flow of water output
Y_{gas}	Gas yield
$F_{gas,\,out}$	Total dry N_2-free volume gas flow produced
$F_{fuel,\,in}$	Mass flow of the input fuel in the gasifier
n_i	Moles of the carbonaceous species in the product gas (CO, CO_2, CH_4),
$n_{C_{in}}$	Total moles of C in the feedstock input
Y_{char}	Char yield
LHV_{gas}	Lower heating value of the product gas
$LHV_{lignite}$	Lower heating value of lignite
m_{char}	Mass of the residual char estimated by the post-combustion in the gasifier
m_{fuel}	Mass of the total fuel fed to the gasifier
X_C	Carbon conversion (%)
η_{CG}	Cold gas efficiency (%)

References

1. Stiegel, G.J.; Maxwell, R.C. Gasification technologies: The path to clean, affordable energy in the 21st century. *Fuel Process. Technol.* **2001**, *71*, 79–97. [CrossRef]
2. Krause, D.; Herdel, P.; Ströhle, J.; Epple, B. HTW^{TM}-gasification of high volatile bituminous coal in a 500 kWth pilot plant. *Fuel* **2019**, *250*, 306–314. [CrossRef]
3. Milne, T.A.; Evans, R.J.; Abatzaglou, N. *Biomass Gasifier "'Tars'": Their Nature, Formation, and Conversion*; National Renewable Energy Laboratory: Golden, CO, USA, 1998.
4. Stec, M.; Czaplicki, A.; Tomaszewicz, G.; Słowik, K. Effect of CO2 addition on lignite gasification in a CFB reactor: A pilot-scale study. *Korean J. Chem. Eng.* **2018**, *35*, 129–136. [CrossRef]
5. Aravind, P.V.; De Jong, W. Evaluation of high temperature gas cleaning options for biomass gasification product gas for Solid Oxide Fuel Cells. *Prog. Energy Combust. Sci.* **2012**, *38*, 737–764. [CrossRef]
6. Sikarwar, V.S.; Zhao, M.; Fennell, P.S.; Shah, N.; Anthony, E.J. Progress in biofuel production from gasification. *Prog. Energy Combust. Sci.* **2017**, *61*, 189–248. [CrossRef]
7. Venvik, H.J.; Yang, J. Catalysis in microstructured reactors: Short review on small-scale syngas production and further conversion into methanol, DME and Fischer-Tropsch products. *Catal. Today* **2017**, *285*, 135–146. [CrossRef]
8. Wang, H.; Pei, Y.; Qiao, M.; Zong, B. Design of bifunctional solid catalysts for conversion of biomass-derived syngas into biofuels. In *Production of Biofuels and Chemicals with Bifunctional Catalysts*; Springer Nature: Singapore, 2017; pp. 137–158, ISBN 9789811051371.
9. Matsuoka, K.; Hosokai, S.; Kato, Y.; Kuramoto, K.; Suzuki, Y.; Norinaga, K.; Hayashi, J.I. Promoting gas production by controlling the interaction of volatiles with char during coal gasification in a circulating fluidized bed gasification reactor. *Fuel Process. Technol.* **2013**, *116*, 308–316. [CrossRef]
10. Benedikt, F.; Fuchs, J.; Schmid, J.C.; Müller, S.; Hofbauer, H. Advanced dual fluidized bed steam gasification of wood and lignite with calcite as bed material. *Korean J. Chem. Eng.* **2017**, *34*, 2548–2558. [CrossRef]
11. Rapagnà, S.; Gallucci, K.; Foscolo, P.U. Olivine, dolomite and ceramic filters in one vessel to produce clean gas from biomass. *Waste Manag.* **2017**. [CrossRef]
12. Devi, L.; Ptasinski, K.J.; Janssen, F.J.J.G. A review of the primary measures for tar elimination in biomass gasification processes. *Biomass Bioenergy* **2002**, *24*, 125–140. [CrossRef]
13. Bayarsaikhan, B.; Sonoyama, N.; Hosokai, S.; Shimada, T.; Hayashi, J.I.; Li, C.Z.; Chiba, T. Inhibition of steam gasification of char by volatiles in a fluidized bed under continuous feeding of a brown coal. *Fuel* **2006**, *85*, 340–349. [CrossRef]
14. Kern, S.; Pfeifer, C.; Hofbauer, H. Gasification of lignite in a dual fluidized bed gasifier - Influence of bed material particle size and the amount of steam. *Fuel Process. Technol.* **2013**, *111*, 1–13. [CrossRef]
15. Karimipour, S.; Gerspacher, R.; Gupta, R.; Spiteri, R.J. Study of factors affecting syngas quality and their interactions in fluidized bed gasification of lignite coal. *Fuel* **2013**, *103*, 308–320. [CrossRef]

16. Herdel, P.; Krause, D.; Peters, J.; Kolmorgen, B.; Ströhle, J.; Epple, B. Experimental investigations in a demonstration plant for fluidized bed gasification of multiple feedstock's in 0.5 MW th scale. *Fuel* **2017**, *205*, 286–296. [CrossRef]

17. LIG2LIQ Eu Project. Available online: https://www.lig2liq.eu/ (accessed on 17 February 2020).

18. Gibilaro, L.G. *Fluidization Dynamics The Formulation and Applications of a Predictive Theory for the Fluidized State*; Butterworth-Heinemann: Oxford, UK, 2001.

19. Magnolithe Steel Industry Products. Available online: http://www.magnolithe.at/pages/en/firma/fa_rohstoffe.htm (accessed on 17 February 2020).

20. Rauch, R.; Pfeifer, C.; Bosch, K.; Hofbauer, H.; Swierczynski, D.; Courson, C.; Kiennemann, A. Comparison of different olivines for biomass steam gasification. *Proc. Conf. Sci. Therm. Chem. Biomass Convers.* **2004**, 799–809.

21. Christodoulou, C.; Grimekis, D.; Panopoulos, K.D.; Pachatouridou, E.P.; Iliopoulou, E.F.; Kakaras, E. Comparing calcined and un-treated olivine as bed materials for tar reduction in fluidized bed gasification. *Fuel Process. Technol.* **2014**, *124*, 275–285. [CrossRef]

22. Michel, R.; Ammar, M.R.; Poirier, J.; Simon, P. Phase transformation characterization of olivine subjected to high temperature in air. *Ceram. Int.* **2013**, *39*, 5287–5294. [CrossRef]

23. Klutz, H.J.; Moser, C.; Block, D.R.P. WTA Fine Grain Drying: Module for Lignite-fired Power Plants of the Future-Development and Operating Results of the Fine Grain Drying Plant. *VGB Power Tech.* **2006**, *86*, 11.

24. Gallucci, K.; Jand, N.; Foscolo, P.U.; Santini, M. Cold model characterisation of a fluidised bed catalytic reactor by means of instantaneous pressure measurements. *Chem. Eng. J.* **2002**, *87*, 61–71. [CrossRef]

25. Gallucci, K.; Gibilaro, L.G. Dimensional cold-modeling criteria for fluidization quality. *Ind. Eng. Chem. Res.* **2005**, *44*, 5152–5158. [CrossRef]

26. Rapagna, S.; D'orazio, A.; Gallucci, K.; Foscolo, P.U.; Nacken, M.; Heidenreich, S. Hydrogen rich gas from catalytic steam gasification of biomass in a fluidized bed containing catalytic filters. *Chem. Eng. Trans.* **2014**, *37*, 157–162.

27. D'Orazio, A.; Rapagnà, S.; Foscolo, P.U.; Gallucci, K.; Nacken, M.; Heidenreich, S.; Di Carlo, A.; Dell'Era, A. Gas conditioning in H2 rich syngas production by biomass steam gasification: Experimental comparison between three innovative ceramic filter candles. *Int. J. Hydrogen Energy* **2015**, *40*, 7282–7290. [CrossRef]

28. Di Marcello, M.; Gallucci, K.; Rapagnà, S.; Gruber, R.; Matt, M. HPTLC and UV spectroscopy as innovative methods for biomass gasification tars analysis. *Fuel* **2014**, *116*, 94–102. [CrossRef]

29. Rapagnà, S.; Gallucci, K.; Di Marcello, M.; Foscolo, P.U.; Nacken, M.; Heidenreich, S.; Matt, M. First Al2O3based catalytic filter candles operating in the fluidized bed gasifier freeboard. *Fuel* **2012**, *97*, 718–724. [CrossRef]

30. Savuto, E.; Di Carlo, A.; Steele, A.; Heidenreich, S.; Gallucci, K.; Rapagnà, S. Syngas conditioning by ceramic filter candles filled with catalyst pellets and placed inside the freeboard of a fluidized bed steam gasifier. *Fuel Process. Technol.* **2019**, *191*, 44–53. [CrossRef]

31. Font Palma, C. Modelling of tar formation and evolution for biomass gasification: A review. *Appl. Energy* **2013**, *111*, 129–141. [CrossRef]

32. Tian, F.J.; Yu, J.; McKenzie, L.J.; Hayashi, J.I.; Li, C.Z. Conversion of fuel-N into HCN and NH3 during the pyrolysis and gasification in steam: A comparative study of coal and biomass. *Energy Fuels* **2007**, *21*, 517–521. [CrossRef]

33. Xie, K.C.; Lin, J.Y.; Li, W.Y.; Chang, L.P.; Feng, J.; Zhao, W. Formation of HCN and NH33 during coal macerals pyrolysis and gasification with CO_2. *Fuel* **2005**, *84*, 271–277. [CrossRef]

34. Chang, L.P.; Xie, Z.L.; Xie, K.C. Study on the formation of NH_3 and HCN during the gasification of brown coal in steam. *Process Saf. Environ. Prot.* **2006**, *84*, 446–452. [CrossRef]

35. Li, C.Z.; Tan, L.L. Formation of NOx and SOx precursors during the pyrolysis of coal and biomass. Part III. Further discussion on the formation of HCN and NH3 during pyrolysis. *Fuel* **2000**, *79*, 1899–1906.

36. Zhou, J.; Masutani, S.M.; Ishimura, D.M.; Turn, S.Q.; Kinoshita, C.M. Release of fuel-bound nitrogen during biomass gasification. *Ind. Eng. Chem. Res.* **2000**, *39*, 626–634.

37. Demirbaş, A.; Aslan, A. Evaluation of lignite combustion residues as cement additives. *Cem. Concr. Res.* **1999**, *29*, 983–987.

38. Ilic, M.; Cheeseman, C.; Sollars, C.; Knight, J. Mineralogy and microstructure of sintered lignite coal fly ash. *Fuel* **2003**, *82*, 331–336.

39. Sathonsaowaphak, A.; Chindaprasirt, P.; Pimraksa, K. Workability and strength of lignite bottom ash geopolymer mortar. *J. Hazard. Mater.* **2009**, *168*, 44–50.

40. Vamvuka, D.; Pitharoulis, M.; Alevizos, G.; Repouskou, E.; Pentari, D. Ash effects during combustion of lignite/biomass blends in fluidized bed. *Renew. Energy* **2009**, *34*, 2662–2671.

41. Galloway, B.D.; Sasmaz, E.; Padak, B. Binding of SO3 to fly ash components: CaO, MgO, Na_2O and K_2O. *Fuel* **2015**, *145*, 79–83.

42. Hu, Y.; Watanabe, M.; Aida, C.; Horio, M. Capture of H_2S by limestone under calcination conditions in a high-pressure fluidized-bed reactor. *Chem. Eng. Sci.* **2006**, *61*, 1854–1863.

43. Toporov, D.; Abraham, R. Gasification of low-rank coal in the High-Temperature Winkler (HTW) process. *J. South. Afr. Inst. Min. Metall.* **2015**, *115*, 589–597.